IJC
International Journal of Cancer

Cannabidiol stimulates Aml-1a-dependent glial differentiation and inhibits glioma stem-like cells proliferation by inducing autophagy in a TRPV2-dependent manner

Massimo Nabissi[1†], Maria Beatrice Morelli[1,2†], Consuelo Amantini[3], Sonia Liberati[2], Matteo Santoni[4], Lucia Ricci-Vitiani[5], Roberto Pallini[6] and Giorgio Santoni[1]

[1] Section of Experimental Medicine, School of Pharmacy, University of Camerino, Camerino, Italy
[2] Department of Molecular Medicine, Sapienza University, Rome, Italy
[3] School of Biosciences and Veterinary Medicine, University of Camerino, Camerino, Italy
[4] Clinica Di Oncologia Medica, AOU Ospedali Riuniti-Università Politecnica Delle Marche, Ancona, Italy
[5] Department of Hematology, Oncology and Molecular Medicine, Istituto Superiore Di Sanità, Rome, Italy
[6] Department of Neurosurgery, Università Cattolica Del Sacro Cuore, Rome, Italy

Glioma stem-like cells (GSCs) correspond to a tumor cell subpopulation, involved in glioblastoma multiforme (GBM) tumor initiation and acquired chemoresistance. Currently, drug-induced differentiation is considered as a promising approach to eradicate this tumor-driving cell population. Recently, the effect of cannabinoids (CBs) in promoting glial differentiation and inhibiting gliomagenesis has been evidenced. Herein, we demonstrated that cannabidiol (CBD) by activating transient receptor potential vanilloid-2 (TRPV2) triggers GSCs differentiation activating the autophagic process and inhibits GSCs proliferation and clonogenic capability. Above all, CBD and carmustine (BCNU) in combination overcome the high resistance of GSCs to BCNU treatment, by inducing apoptotic cell death. Acute myeloid leukemia (Aml-1) transcription factors play a pivotal role in GBM proliferation and differentiation and it is known that Aml-1 control the expression of several nociceptive receptors. So, we evaluated the expression levels of Aml-1 spliced variants (Aml-1a, b and c) in GSCs and during their differentiation. We found that Aml-1a is upregulated during GSCs differentiation, and its downregulation restores a stem cell phenotype in differentiated GSCs. Since it was demonstrated that CBD induces also TRPV2 expression and that TRPV2 is involved in GSCs differentiation, we evaluated if Aml-1a interacted directly with TRPV2 promoters. Herein, we found that Aml-1a binds TRPV2 promoters and that Aml-1a expression is upregulated by CBD treatment, in a TRPV2 and PI3K/AKT dependent manner. Altogether, these results support a novel mechanism by which CBD inducing TRPV2-dependent autophagic process stimulates Aml-1a-dependent GSCs differentiation, abrogating the BCNU chemoresistance in GSCs.

Cancer Cell Biology

Key words: glioblastoma stem-like cells, cannabidiol, differentiation, Aml-1, autophagy, chemosensitivity

Abbreviations: Abs: antibodies; Aml-1: acute myeloid leukemia; AKT: Protein kinase B; BAF1: bafilomycin A1; bFGF: basic fibroblast growth factor; β_{III}-tubulin: class III beta-tubulin; BCNU: carmustine; BrdU: 5-bromo-2-deoxyuridine; CB: cannabinoid; CBD: cannabidiol; ChIP: chromatin immunoprecipitation; CPZ: capsazepine; CXCR4: C-X-C chemokine receptor type 4; D-GSCs: differentiated GSCs; EGF: epidermal growth factor; eiF: eukaryotic initiator factors; FACS: fluorescence activated cell sorting analysis; FBS: fetal bovine serum; FITC: fluorescein isothiocyanate; GAPDH: glyceraldehyde-3-phosphate dehydrogenase; GFAP: glial fibrillary acidic protein; GSCs: glioblastoma stem-like cells; HRP: horseradish peroxidase; JC-1: 5,5',6,6'-tetrachloro-1,1',3,3'-tetraehylbenzimidazolylcarbocyanineiodide; 3-MA: 3-methyladenine; LC3: microtubuled-associated protein-1 light chain 3; $\Delta\Psi$m: mitochondrial transmembrane potential; MTT: 3-(4,5-dimethylthazol-2-yl)-2,5-diphenyl tetrazolium bromide; Oct-4: octamer-binding transcription factor 4; PI: propidium iodide; qRT-PCR: quantitative real-time polymerase chain reaction; RR: ruthenium red; TMZ: temozolomide; TRP: transient receptor potential; TRPV: transient receptor potential vanilloid channel; TRPV2: transient receptor potential vanilloid type 2; siGLO: non-targeting siRNA with at least four mismatches to any human gene used as negative control; siAml-1: four RNA duplex targeting Aml-1 gene; siAml-1a: consisting of three RNA duplex targeting Aml-1a spliced variant; Sox2: sex determining region Y-box 2; SSEA-1: 3-fucosyl-N-acetyllactosamine.

Additional Supporting Information may be found in the online version of this article.

[†]M.N. and M.B.M. contributed equally to this work

Grant sponsor: Italian Minister of Research; Grant number: PRIN2010; Grant sponsor: FIRC (National Grant 2011–2013); **Grant number:** 11095

DOI: 10.1002/ijc.29573

History: Received 16 Oct 2014; Accepted 15 Apr 2015; Online 21 Apr 2015

Correspondence to: Dr. Massimo Nabissi, School of Pharmacy, University of Camerino, Camerino (MC), Italy, Tel.: +390737403306, Fax: +390737403325, E-mail: massimo.nabissi@unicam.it

What's new?

Glioma stem-like cells (GSCs) are a cell subpopulation that is believed to be involved in glioblastoma multiforme tumor initiation and acquired chemoresistance. This study shows that cannabidiol acts on GSCs via the Transient Receptor Potential Vanilloid-2 (TRPV2) channel to induce autophagic-dependent inhibition of proliferation, promotion of differentiation, and sensitization to the cytotoxic effects of alkylating agents. Moreover, the authors identify a transcriptional network that is induced by cannabidiol via the Aml-1a transcription factor and stimulates TRPV2-dependent inhibition of proliferation and promotion of differentiation in GSCs. The results suggest a promising approach for regulating the tumor stem-like cell compartment in glioblastoma.

Glioblastoma multiforme (GBM) remains the most deadly human brain tumor, with a median survival of approximately 1 year.[1] GBM presents unique challenges to therapy due to its location, aggressive biological behavior and diffuse infiltrative growth. Despite the development of new surgical techniques, radiotherapy and the use of multiple antineoplastic drugs, a cure for GBM remains elusive.[2,3] Recent studies have led to the hypothesis that GBM is maintained by a small population of glioma stem-like cells (GSCs), isolated from both glioma tissues and glioma cell lines.[4] GSCs retain stem cell properties, are highly tumorigenic, and display increased resistance to radiation and conventional chemotherapeutic drugs, as carmustine (bis-chloroethylnitrosourea, BCNU) and temozolomide (TMZ), thus GSCs are potential key target for novel GBM therapies.[4–7] Recent reports support prodifferentiation as a potential strategy to inhibit GSCs tumorigenicity and activation of the autophagic process was found to promote GSCs differentiation and to increase radio and chemosensitivity.[8,9] Cannabinoids, as Δ9-tetrahydrocannabinol (THC) and cannabidiol (CBD), were found to inhibit human glioma cell lines viability.[10,11] THC and cannabinoid agonists (HU210, JWH133) were found to induce autophagy and stimulate GSCs differentiation by cannabinoid receptors (CBR).[10,12,13] Autophagic process is regulated by different autophagy-related genes (ATGs) and signaling molecules such as mTOR, AKT and class I and III phosphatidyl-inositol 3-kinase.[9] At molecular levels THC and CBD regulate different key genes involved in autophagic process, as Beclin-1 and AKT signaling in glioma cell lines,[10] while no data about CBD in regulating autophagy in GSCs were actually provided.

Previously, we have demonstrated that transient receptor potential vanilloid type 2 (TRPV2), a target receptor for CBD, impairs GSC proliferation and promotes astroglial differentiation *in vitro* and *in vivo*.[14]

The transcriptional network regulating GSCs proliferation and differentiation is still partially identified, indicating some drivers of tumor initiation, as the Runt-related transcription factor 1 (RunX-1), named Acute myeloid leukemia 1 (Aml-1) in human.[15,16]

Aml-1 gene generates at least three alternatively spliced variants: Aml-1a, -b and -c. Aml-1b and Aml-1c possess the DNA-binding region and the transcriptional regulatory domains and they are considered similar in functions. Otherwise, Aml-1a retains the DNA-binding domain but lacks the transcriptional regulatory domains and it is considered a potential functional antagonist of Aml-1b and Aml-1c.[17] Aml-1 gene has been reported mutated in human cancer, as somatic point mutations in myelodysplasia and chromosomal translocation in acute myeloid leukaemia.[18,19] Aberrant expression in breast and Aml-1 deletion in esophagus adenocarcinoma have been documented.[20,21] Aml-1 was also found expressed in human GBM cell lines[15] but no information on the role of Aml-1 and its spliced variants in GBM was defined. In brain, Aml-1 plays a relevant role in sensory neuron differentiation, controlling the expression of several sensory nociceptive receptors, including members of the transient receptor potential (TRP) class of thermal receptors.[22,23]

Herein, we provide the first evidence on the role of TRPV2 in autophagic-dependent astroglial GSCs differentiation. In addition, we found that the Aml-1a spliced variant is upregulated during GSCs differentiation, and that its downregulation restores a stem cell phenotype and proliferation in differentiated GSCs. Finally, we evidenced that Aml-1a promotes TRPV2 expression, and that Aml-1a is upregulated by CBD.

Material and Methods

Cell cultures

GSC lines (#1, #30 and #83) previously characterized[11] were isolated from surgical samples of three adult patients, diagnosed according to the WHO classification of tumors of the central nervous system, who had undergone craniotomy at the Institute of Neurosurgery, Catholic University School of Medicine, Rome. Informed consent was obtained before surgery according to the protocols approved. GSC lines were cultured in a serum-free medium supplemented with 20 ng/ml of epidermal growth factor (EGF) and 10 ng/ml of basic fibroblast growth factor (bFGF). For differentiation, GSC lines were grown in medium supplemented with 5% fetal bovine serum (FBS).

Reagents and antibodies

Cannabidiol (CBD, >98% purity), ruthenium red (RR), capsazepine (CPZ, >99% purity), AM251 (>99% purity), AM630 (>98% purity) and GW9662 (>98% purity) were purchased from Tocris Bioscience (Bristol, UK). 5-bromo-2-deoxyuridine (BrdU, ≥99% purity), 1,3-bis (2-chloroethyl)-1-nitrosurea (BCNU, ≥98% purity) and 3-methyladenine (3-MA, ≥98% purity) were obtained from Sigma Aldrich (St. Louis, MO). Bafilomycin A1 (BAF1, ≥90% purity) was from Labogen (Milan, Italy). Rapamycin

(≥98% purity) was from Adipogen (San Diego, CA). The following mouse monoclonal antibodies (mAbs) were used: anti-glyceraldehyde-3-phosphate dehydrogenase (GAPDH)-peroxidase (Sigma Aldrich), anti-class III beta-tubulin (β_{III}-tubulin) (Millipore, Billerica, MA), anti-Aml-1 (Cell Signaling Technology, Danvers, MA) and fluorescein isothiocyanate (FITC)-conjugated anti-BrdU (Becton Dickinson Biosciences, San Jose, CA). The following polyclonal Abs were used: rabbit anti-AKT (Cell Signaling), rabbit anti-pAKT (Cell Signaling), mouse anti-CD133-PE (Miltenyi, Bergisch, Germany), mouse anti-CXCR4- Pe-cy5 (eBioscience, Hatfield, UK), rabbit anti-glial fibrillary acidic protein (GFAP), rabbit anti-nestin (Sigma-Aldrich), rabbit anti-Oct-4 (Cell Signaling), mouse anti-SSEA-1-PE (eBioscience), goat anti-Sox2 (R&D System, Minneapolis, MN), goat anti-TRPV2 (Santa Cruz Biotechnology, Heidelberg, Germany), rabbit anti-microtubule-associated protein-1 light chain 3 (LC3, Novus Biological, Littleton, CO), rabbit anti-Beclin-1 (Cell Signaling Technology), rabbit anti-Aml-1-Chip grade (Abcam plc, Cambridge, UK), rabbit Control IgG-CHIP grade (Abcam), rabbit anti-RNA Polymerase II (Qiagen, Milan, Italy), rabbit anti-TFIIB (Abcam). The following secondary antibodies were used: horseradish peroxidase (HRP)-conjugated sheep anti-mouse IgG, HRP-conjugated donkey anti-goat IgG (Santa Cruz Biotechnology) and HRP-conjugated donkey anti-rabbit IgG (GE Healthcare, Munich, Germany), PE-conjugated anti-rabbit (Santa Cruz Biotechnology), PE-conjugated anti-goat (Santa Cruz Biotechnology), PE-conjugated anti-mouse (Santa Cruz Biotechnology). The following isotypes were used: PE-conjugated Mouse IgG1 (Miltenyi), PE-cy5-conjugated mouse IgG2Ak (eBioscience), PE-conjugated mouse IgM (eBioscience).

Cell viability

Cell viability was assessed by the 3–(4,5-dimethylthazol-2-yl)-2,5-diphenyl tetrazolium bromide (MTT) assay as previously described.[11] 3×10^4 cells in 100 μl were seeded in 96-well plates. After 24 hr of incubation, compounds or vehicles were added. Four replicates were used for each treatment. The absorbance of the samples against a background control (medium alone) was measured at 570 nm using an ELISA reader microliter plate (BioTek Instruments, Winooski, VT).

Soft agar assay

Sphere-forming/self-renewal capability was tested by soft agar assay in six-well plate. Briefly, a 500 μl underlayer of 0.6% soft agarose (sea plaque agarose diluted in medium plus growth factors) was prepared in each 35-mm well. A total of 3×10^3 cells/well were added above the layer as a second layer composed of 2/3 soft agarose 0.4% and 1/3 cells plus medium in a total volume of 500 μl. The plates were incubated for 10 min at 4 °C and for 15 days at 37 °C. Then, the dishes were stained with 70 μl of Crystal Violet (0.1%) and colonies were counted.

BrdU cell proliferation assay

The incorporation of BrdU was assessed using the BrdU Cell Proliferation Assay (Millipore). 3×10^4 cells in 100 μl were seeded in 96-well plates and treated with vehicle or CBD. Incorporated BrdU was detected by adding the peroxidase substrate, following manufactoring protocol. Spectrophotometric detection was performed at a dual wavelength of 450/550 nm using an ELISA reader microliter plate. In some experiment, cells labeled with 20 μM BrdU were fixed with 4% paraformaldehyde and stained with anti-BrdU FITC-conjugated Ab as previously described.[14]

Cell cycle analysis

3×10^5 cells/ml were incubated with the appropriate drugs for 24 hr, in six-wells plates. Cells were fixed in ice-cold 70% ethanol, treated for 30 min at 37 °C with 100 μg/ml ribonuclease A solution (Sigma-Aldrich), stained for 30 min at room temperature with propidium iodide (PI) 20 μg/ml (Sigma-Aldrich) and analyzed by flow cytometry using linear amplification.

Apoptosis assays

The exposure of phosphatidylserine was detected by Annexin-V staining. 3×10^5 cells/ml were seeded in six-wells plates and treated with different doses of the appropriate drugs for 24 hr. Four replicates were used for each treatment. After treatment, cells were stained with 5 μl of Annexin-V FITC (Enzo Life Sciences, Farmingdale, NY) for 10 min at room temperature and analyzed on a FACScan flow cytometer using CellQuest software, as previously described.[11]

PI incorporation assay

3×10^5 cells/ml were seeded in six-wells plates and treated with different doses of CBD for 24 hr. After treatment the cells were incubated in medium containing 20 μg/ml PI for 10 min at room temperature. The cells were then analyzed by flow cytometry using CellQuest software.

Western blot analysis

3×10^5 cells/ml were seeded in six-wells plates and treated with different doses of the appropriate drugs. Total proteins from GSC lines were obtained as previously described.[14] Plasma membrane, cytosol and nuclear fractions were isolated using the Subcellular Protein Fractionation kit (Thermo Scientific, Rockford, IL), according to the manufacturer's directions. 20 μg of the lysate was separated on a SDS-polyacrylamide gel, transferred onto Hybond-C extra membranes (GE Healthcare), blocked with 5% low-fat dry milk in PBS-Tween 20, immunoblotted with LC3 (2 μg/mL), Beclin-1 (1:1,000), GFAP (1:300), β_{III}-tubulin (1:1,000), Nestin (1:1,000), Sox2 (0.5 μg/mL), anti-Aml-1 (1:1,000), anti-AKT (1:1,000), anti-pAKT (1:1,000) and anti-TRPV2 (1:200) followed by the appropriate HRP-conjugated secondary Abs (1:2,000). For quantification, anti-GAPDH (1:5,000) or anti-TFIIB (4 μg/ml) Abs was used as loading control. The detection was performed using the LiteAblot ®PLUS or the LiteAblot ®TURBO (EuroClone, Milan, Italy) kits and densitometric analysis was carried out by a Chemidoc using the Quantity One software (Bio-Rad).

Mitochondrial transmembrane potential

Mitochondrial transmembrane potential ($\Delta\Psi_m$) was evaluated by 5,5',6,6'-tetrachloro-1,1',3,3'-tetraehylbenzimidazolylcarbocyanineiodide (JC-1) staining. 3×10^5 cells/ml were seeded in six-wells plate and treated with the appropriate drugs for 24 hr and then incubated for 10 min at room temperature with 10 μg/ml of JC-1. Carbonyl cyanide chlorophenylhydrazone protonophore (CCCP, 50 μg), a mitochondrial uncoupler that collapses the $\Delta\Psi_m$ was used as a positive control. JC-1 was excited by an argon laser (488 nm), and the green (530 nm)/red (570 nm) emission fluorescence was collected simultaneously. Samples were analyzed using a FACScan cytofluorimeter with CellQuest software.

Fluorescence-activated cell sorting analysis

3×10^5 cells/ml were seeded in six-wells plate and treated with the appropriate drugs. GSC lines were labeled with anti-CD133 (1:10), anti-Oct-4 (1:600), anti-SSEA-1 (0.5 μg/10^6 cells), anti-Nestin (1:50), anti-Sox2 (1:50), anti-CXCR4 (1:50), anti-GFAP (1:100), anti-β_{III}-tubulin (1:50), anti-TRPV2 (1:25) Abs, followed by FITC-conjugated or PE-conjugated secondary Abs, where necessary. The specificity of staining was confirmed using isotype-specific Abs as negative control. Samples were analyzed by a FACScan cytofluorimeter using the CellQuest software (Becton Dickinson). Fluorescence intensity was expressed in arbitrary units on logarithmic scale.

Gene expression analysis

Total RNA was extracted with the RNeasy Mini Kit (Qiagen), and cDNA was synthesized using the High-Capacity cDNA Archive Kit (Applied Biosystems, Foster City, PA) according to the manufacturer's instructions. Qualitative PCR were performed using 50 ng of cDNA diluted in PCR master mix (Promega; Supporting Information Table S1). The thermal cycler profile was: 5 min at 95 °C, 35 cycles at 10 sec 95 °C, 20 sec 60 °C, 25 sec 72 °C, followed by 5 min at 72 °C. PCR products were analyzed in a 1.5% agarose gel electrophoresis. Quantitative real-time polymerase chain reactions (qRT-PCR) for CB1, CB2, TRPV1, TRPV2, GPR55, PPARγ, Beclin-1 and Aml-1a, b and c were performed using the iQ5 Multicolor Real-Time PCR Detection System (Bio-Rad, Hercules, CA) as described.[11] All samples were assayed in triplicates in the same plate. Measurement of β-actin levels was used to normalize mRNA contents, and receptors levels were calculated by the $2^{-\Delta\Delta Ct}$ method.

Genes silencing

IBONI siRNA 4-duplexes pools for Aml-1 (siAml-1) isoforms, 3-siRNA duplexed bundle S pools for Aml-1a (siAml-1a) isoform and four siRNA duplexed for Beclin-1 were purchased (Riboxx Life Science, Germany; Supporting Information Table S2). siCONTROL non-targeting siRNA (siGLO) used as negative control and siGLO RISC-Free siRNA (siFLUO, a siRNA non-target Cy3-labeled control siRNA cotransfected with functional siRNA) were purchased from Thermo Scientific-Dharmacon (Lafayette, CO). For gene silencing experiments, GSC lines were plated at the density of 3×10^4/ml in six-wells plates and incubated in differentiation medium for 7 days in presence of 160 pmol of siAml-1, siAml-1a, siBeclin-1, siGLO or siFLUO, following the METAFECTENE SI PRO transfection protocol (Biontex Laboratories, San Diego, CA).

Chromatin immunoprecipitation assay

Chromatin immunoprecipitation (ChIP) studies were performed using EPItech One day kit (Qiagen) following manufacturing protocol. For each ChIP assay chromatin from $\sim 3 \times 10^6$ cells was fragmented to an average size from ~500 to 1,500 bp by eight rounds of sonication (Power: 0.5 W, Time: 2 sec on, 15 sec off; total time 16 sec) in 2 ml tubes using the Sonicator 3000 (MISONIX, Part # 3000) (QSonica, LLC, Newtown, CT). The fragmented chromatin was immunoprecipitated, using 4 μg of anti-Aml-1 Ab-CHIP grade or 4 μg of rabbit control IgG-CHIP grade as negative control or 4 μg of anti-RNA Polymerase II as positive control, by incubation on rotator at +4 °C overnight. Then, the DNA was purified from the precipitated samples using QIAquick MinElute (Qiagen) columns, and analyzed by SYBR green real time PCR using EpiTect ChIP qPCR Assay (Qiagen) with specific primers against the proximal region of human TRPV2 gene promoter sequence (NM_016113.3 (+)08Kb, (+)01Kb), human GAPDH (NM_002046.3 (+)01Kb) and human IGX1A (NC_000012.11(-)01A), according to manufacturer instructions. Data analysis were performed using ChIP qPCR Data Analysis Template (Qiagen). The specificity of Aml-1a in regulating TRPV2 promoters activity was assessed by ChIP analysis and ChIP qPCR Assay comparing TRPV2 promoters expression levels in siAml-1 D-GSCs with siAml-1a D-GSCs lines.

qRT-PCR and PCR array

The Human Autophagy and Stem cell Signaling Pathway Finder PCR Arrays with related reagents were purchased from SABiosciences (Frederick, MD). Total RNA from untreated or GSCs treated for 6 hr with vehicle- or CBD in proliferative medium, and from siGLO- and siAml-1a-transfected differentiated GSC (D-GSC) lines at day 7 post-transfection in differentiative medium, was extracted. 2 μg of total RNA from each sample were subjected to reverse transcription in a total volume of 20 μl using the ReactionReady first strand cDNA (SABiosciences). cDNAs were analyzed by qRT-PCR performed using a IQ5 Multicolor Real time PCR Detection system, the SuperArray's RT2 real-time SYBR Green PCR Master Mix and the relative array, according to manufacturer's instructions. Measurement of two housekeeping genes (GAPDH; Ribosomal protein, large, P0; RPLP0) on the samples was used to normalize mRNA content. The gene expression levels of CBD-treated GSCs or siAml-1a-transfected GSCs were expressed as relative fold compared with untreated or vehicle-treated GSCs or siGLO-transfected D-GSCs. Data acquisition was performed using the web-based integrated PCR Array Data Analysis Tem-235 plate provided by SABiosciences.

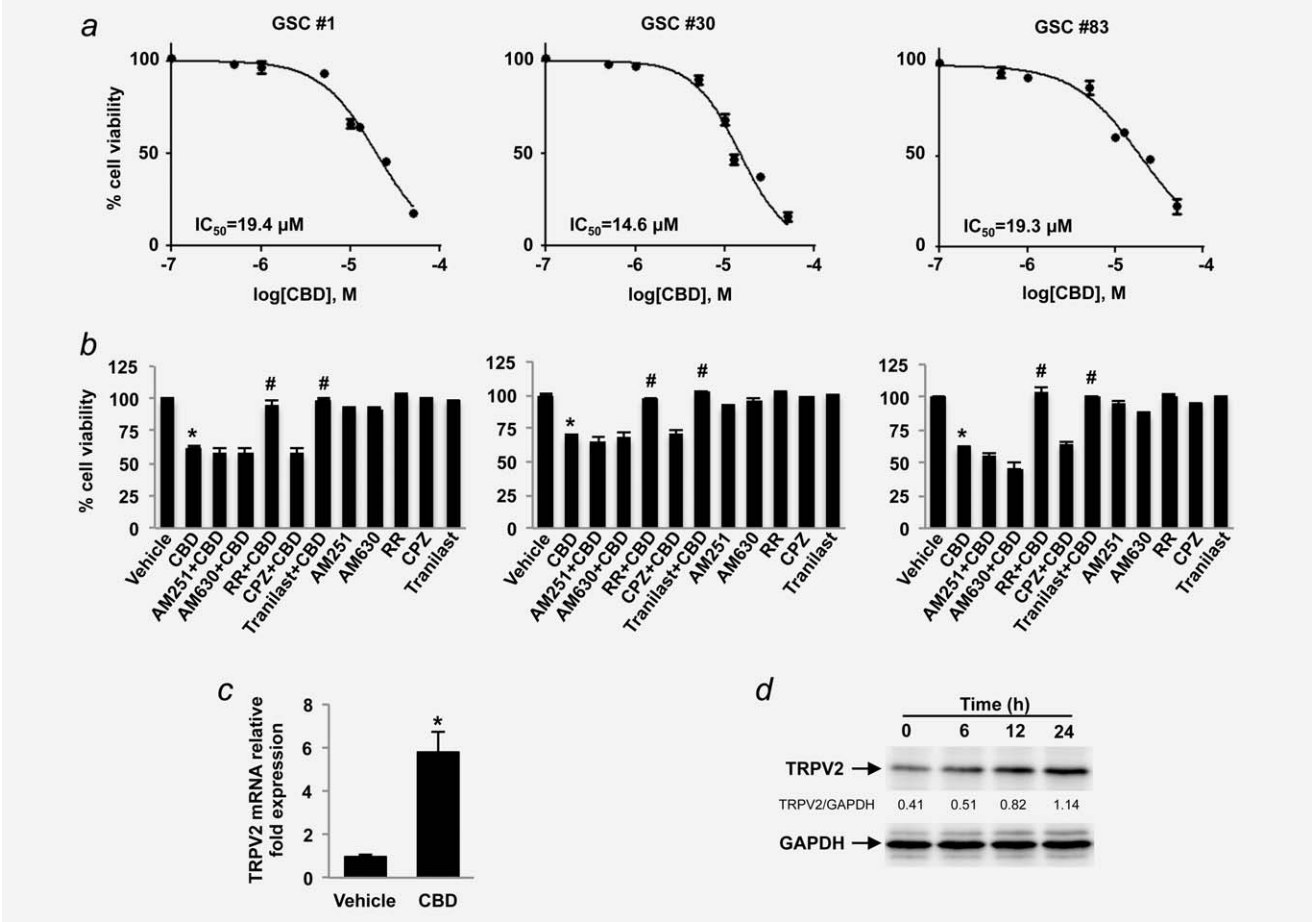

Figure 1. Effect of CBD on GSC cell lines viability. (*a*) GSC #1, #30 and #83 cell lines were cultured for 24 hr with different doses of CBD. Cell viability was determined by MTT assay. Data shown are expressed as mean ± SE of three separate experiments. (*b*) GSC #1, #30 and #83 cells were pretreated with AM251 (10 μM), AM630 (10 μM), RR (25 μM), CPZ (1 μM) and tranilast (50 μM) for 1 hr and then cultured for 24 hr with CBD (10 μM). Cell viability was determined by MTT assay. Data shown are expressed as mean ± SD of three separate experiments; $^{*}p < 0.01$ CBD *vs*. vehicle. $^{\#}p < 0.01$ treatments *vs*. CBD. (*c*) The relative TRPV2 mRNA expression in GSC #83 cells treated with vehicle or 10 μM CBD was evaluated by qRT-PCR. TRPV2 mRNA levels were normalized for β-actin expression. Data are expressed as mean ± SD. $^{*}p < 0.01$ *vs*. vehicle. (*d*) Lysates from GSC #83 cells treated with 10 μM CBD were separated on 7% SDS-PAGE and probed with anti-TRPV2 and anti-GAPDH Abs, respectively. Blots are representative of one of three separate experiments. Numbers represent the densitometric analysis as compared with GAPDH. Data shown are relative to GSC #83 line and are representative of the three GSC lines analyzed.

DNA methylation analysis

The assessment of the methylation status of MGMT promoter was performed in GSC lines, using DNA modification and AMPLI-MGMT kit (Diachem, Naple, IT), following manufacturer instructions. Before Methylation-specific PCR assay, genomic DNA was extracted using DNA extraction kit (Qiagen) and subjected to sodium Bisulfite Conversion of Unmethylated Cytosines using EpiTech Bisulfite kit (Qiagen). PCR products were separated by 2% agarose gel electrophoresis in the presence of ethidium bromide and visualized under UV illumination.

Statistical analysis

The data presented represent the mean and standard deviation (SD) of at least 3 independent experiments. The statistical significance was determined by analysis of variance (ANOVA) or Student's *t test*; *, $^{\#}p < 0.01$. The statistical analysis of IC50 levels was performed using Prism 5.01 (Graph Pad). Data from untreated cells were omitted because no differences were observed between vehicle-treated and untreated cells.

Results

CBD affects GSC lines viability in a TRPV2-dependent manner

GSC lines (#1, #30, #83) were treated with CBD (from 0.5 to 50 μM) up to three days and cell viability was analyzed by MTT assay. CBD induced a significant decrease of cell viabilty (Supporting Information Fig. S1) with an IC_{50} of 19.4 μM (#1), 14.6 μM (#30) and 19.3 μM (#83) at 24 hr post-treatment (Fig. 1*a*). The lowest effective dose of CBD (10 μM) was used for the subsequent experiments. Then we evaluated the expression of CB1 and CB2, and CB-related receptors, such as TRPV1, TRPV2, GPR55 and PPARγ in GSC lines, by qRT-PCR. The results demonstrated the expression of the CB1, CB2, TRPV1 and

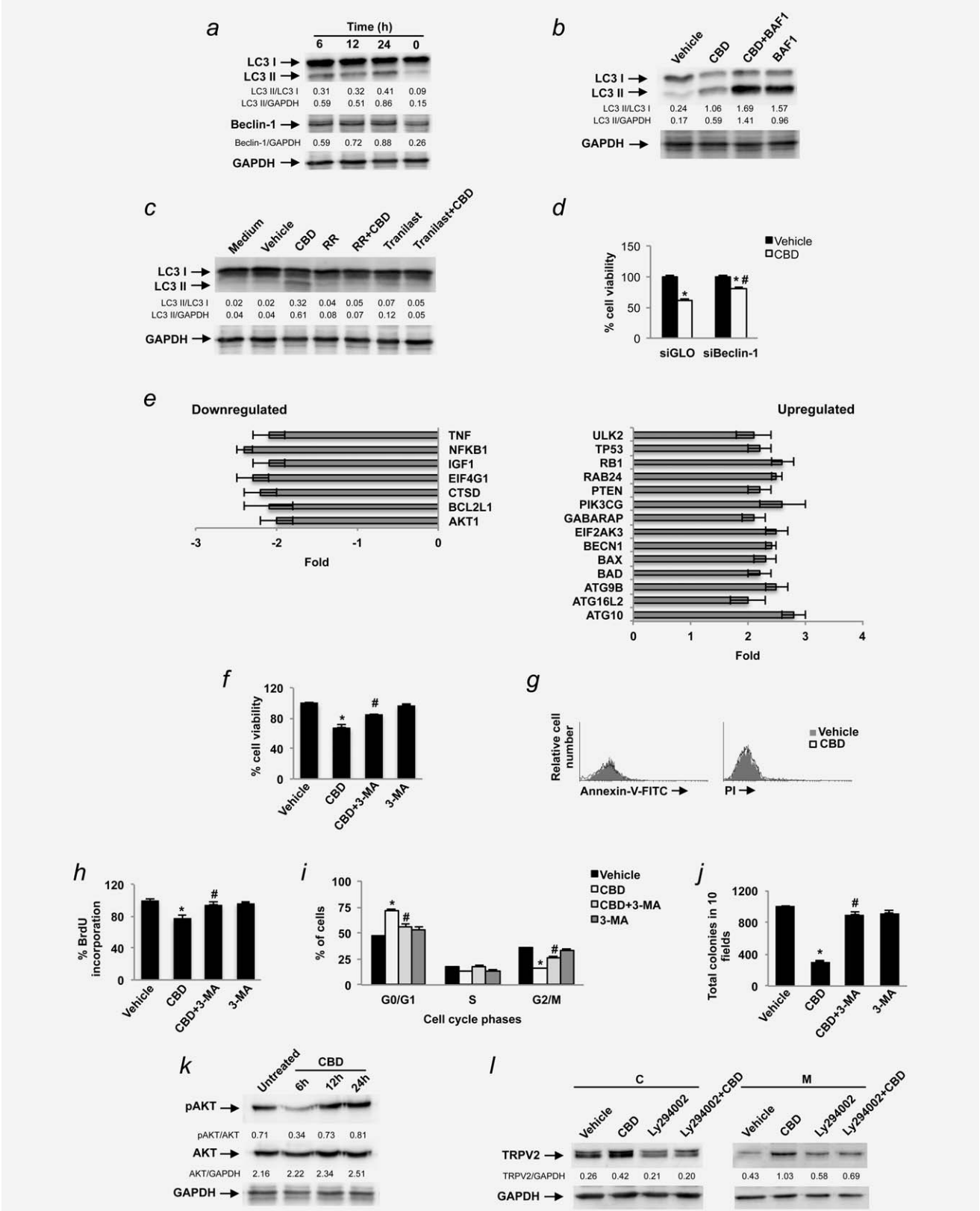
a
Time (h)
6 12 24 0
LC3 I
LC3 II
LC3 II/LC3 I 0.31 0.32 0.41 0.09
LC3 II/GAPDH 0.59 0.51 0.86 0.15
Beclin-1
Beclin-1/GAPDH 0.59 0.72 0.88 0.26
GAPDH
b
Vehicle
CBD
CBD+BAF1
BAF1
LC3 I
LC3 II
LC3 II/LC3 I 0.24 1.06 1.69 1.57
LC3 II/GAPDH 0.17 0.59 1.41 0.96
GAPDH
c
Medium
Vehicle
CBD
RR
RR+CBD
Tranilast
Tranilast+CBD
LC3 I
LC3 II
LC3 II/LC3 I 0.02 0.02 0.32 0.04 0.05 0.07 0.05
LC3 II/GAPDH 0.04 0.04 0.61 0.08 0.07 0.12 0.05
GAPDH
d
Vehicle
CBD
% cell viability
150
100
50
0
siGLO
siBeclin-1
e
Downregulated
TNF
NFKB1
IGF1
EIF4G1
CTSD
BCL2L1
AKT1
-3 -2 -1 0
Fold
Upregulated
ULK2
TP53
RB1
RAB24
PTEN
PIK3CG
GABARAP
EIF2AK3
BECN1
BAX
BAD
ATG9B
ATG16L2
ATG10
0 1 2 3 4
Fold
f
% cell viability
120
80
40
0
Vehicle
CBD
CBD+3-MA
3-MA
g
Relative cell number
Vehicle
CBD
Annexin-V-FITC
PI
h
% BrdU incorporation
120
80
40
0
Vehicle
CBD
CBD+3-MA
3-MA
i
% of cells
100
75
50
25
0
Vehicle
CBD
CBD+3-MA
3-MA
G0/G1
S
G2/M
Cell cycle phases
j
Total colonies in 10 fields
1200
800
400
0
Vehicle
CBD
CBD+3-MA
3-MA
k
Untreated
CBD
6h
12h
24h
pAKT
pAKT/AKT 0.71 0.34 0.73 0.81
AKT
AKT/GAPDH 2.16 2.22 2.34 2.51
GAPDH
l
C
M
Vehicle
CBD
Ly294002
Ly294002+CBD
TRPV2
TRPV2/GAPDH 0.26 0.42 0.21 0.20 0.43 1.03 0.58 0.69
GAPDH

Figure 2:

TRPV2 mRNA (Supporting Information Fig. S2), but not of the GPR55 and PPAR-γ mRNA (data not shown). Thereafter, the involvement of these expressed receptors in CBD-mediated effects, was evaluated by pretreating for 1 hr the GSC lines with 10 μM AM251 (CB1 selective antagonist), 10 μM AM630 (CB2 selective antagonist), 10 μM RR (TRP channel blocker), 10 μM CPZ (TRPV1 selective antagonist) and 50 μM tranilast (TRPV2 selective antagonist), before the addition of 10 μM CBD, one day post-treatment by MTT assay. The results showed that only RR and tranilast are able to revert the CBD effects (Fig. 1*b*), indicating that in GSC lines, CBD inhibits viability in a CB1-, CB2- and TRPV1-independent but TRPV2-dependent manner.

Moreover, by qRT-PCR and western blot analysis we showed a significant increase of TRPV2 expression after treatment with CBD (up to 24 hr) in GSC lines (Figs. 1*c* and 1*d*).

CBD induces TRPV2-dependent autophagy in GSCs

To determine whether the TRPV2-dependent CBD-mediated effects in reducing GSC viability was due to activation of autophagy, we examined the conversion of the soluble form of LC3 (LC3-I) to the lipidated and autophagosome-associated form (LC3-II) and the levels of the autophagy-related protein Beclin-1.[24] We found that CBD increases the cleaved LC3-II form levels (evaluating both LC3-I/LC3-II and LC3-II/GAPDH ratios) and the autophagy-related protein Beclin-1 (Fig. 2*a*). To confirm the ability of CBD to stimulate the autophagy, a dynamic evaluation of this process was performed by the autophagic flux. Pretreatment of GSCs with 50 nM BAF1, which blocks the last steps of autophagic degradation, enhanced the CBD-induced accumulation of LC3-II protein in CBD plus BAF1-treated GSCs, compared with single CBD or BAF1 treatments (Fig. 2*b*). Then, the involvement of TRPV2, in CBD-induced autophagy, was evaluated by treating GSCs with RR and tranilast alone or in combination with CBD. The results showed that both RR and tranilast treatments are able to completely revert the CBD-induced LC3 cleavage (Fig. 2*c*). To evidence that the CBD effect was mediated by autophagic pathway, we knocked-down Beclin-1 gene (Supporting Information Fig. S3) and the CBD-mediated effect was determined by MTT assay in siBeclin-1- and siGLO-transfected GSC lines. As shown, the decrease of cell viability observed with CBD treatment, was significantly reverted in siBeclin-1- compared with siGLO-transfected GSC lines (Fig. 2*d*), suggesting a role of autophagic machinery in regulating CBD effects in GSC lines.

The molecular mechanism underlying the CBD-mediated autophagic process, was evaluated by Autophagy Signaling Pathway Finder PCR array analysis in GSCs cells 6 hr post-treatment. The results showed that CBD was able to modulate the expression of different genes regulating the autophagic and apoptotic processes, as compared with vehicle-treated GSCs (Fig. 2*e*, Supporting Information Table S3).

Furthermore, we evaluated the role of the autophagic process in the TRPV2-mediated inhibition of GSC viability by using the autophagic inhibitors, 3-MA (5 mM) or (50 nM) BAF1. We found that CBD inhibits the viability (Fig. 2*f*), BrdU incorporation (Fig. 2*h*, Supporting Information Fig. S4) and arrests the cell cycle at the G0/G1 phase (Fig. 2*i*), without inducing cell death (Fig. 2*g*). Moreover, these CBD-mediated effects were completely reverted by 3-MA (Figs. 2*f-i*) and BAF1 (data not shown).

Figure 2. CBD activates the autophagic pathway. (*a*) Lysates from GSC #83 cells, untreated or treated with 10 μM of CBD, were separated on 14% or 10% SDS-PAGE and probed with anti-LC3 or anti-Beclin-1 Abs, respectively, and anti-GAPDH Ab. Blots are representative of one of three separate experiments. Numbers represent the densitometric analysis. (*b*) Lysates from GSC #83 cells, pretreated with BAF1 (50 nM) for 1 hr and then treated with 10 μM of CBD or vehicle for 24 hr, were separated on 14% SDS-PAGE and probed with anti-LC3 and anti-GAPDH Abs. Blots are representative of one of three separate experiments. Numbers represent the densitometric analysis. (*c*) Lysates from GSC #83 cells, untreated or pretreated with RR (10 μM) and tranilast (50 μM) for 1 hr and then treated with 10 μM of CBD or vehicle for 24 hr, were separated on 14% SDS-PAGE and probed with anti-LC3 and anti-GAPDH Abs. Blots are representative of one of three separate experiments. Numbers represent the densitometric analysis. (*d*) siGLO GSCs and siBeclin-1 GSCs were cultured for 24 hr with vehicle or 10 μM CBD. Cell viability was determined by MTT assay. Data shown are expressed as mean ± SD of three separate experiments; $*p < 0.01$ *vs*. vehicle-treated cells; $\#p < 0.01$ CBD-treated siBeclin-1 GSCs *vs*. CBD-treated siGLO GSCs. (*e*) Autophagy RT profiler PCR array in mRNA samples extracted from GSCs treated for 6 hr with vehicle or 10 μM of CBD. Values represent fold differences of individual gene expression in CBD- compared to vehicle-treated GSCs. The expression levels were normalized to the average Ct value of two housekeeping genes (GAPDH and RPLP0) and calculated by the ΔΔCt method. Graphs include genes whose expression is, at least, 2-fold regulated. (*f*) GSC #83 cells were pretreated with 3-MA (5 mM) for 1 hr and then cultured for 24 hr with CBD 10 μM or vehicle. Cell viability was determined by MTT assay. Data are expressed as mean ± SD; $*p < 0.01$ *vs*. vehicle; $\#p < 0.01$ *vs*. CBD-treated cells. (*g*) Annexin-V+ and PI+ cells were determined in GSCs treated with vehicle or CBD for 24 hr by FACS analysis. Histograms are representative of one of three separate experiments. (*h*) GSCs #83 were treated as above described and proliferation was assessed with the BrdU incorporation assay. The percentage values of BrdU incorporation was reported respect to the vehicle OD. Data are expressed as mean ± SD. $*p < 0.01$ *vs*. vehicle; $\#p < 0.01$ *vs*. CBD-treated cells. (*i*) GSCs #83 were cultured as above described and stained with PI solution to assess the cell cycle distribution pattern. The values were expressed as the mean ± SD of the cells percentage in each phase. $*p < 0.01$ *vs*. vehicle; $\#p < 0.01$ *vs*. CBD-treated cells. (*j*) GSCs were grown in soft agar for 14 days and treated with vehicle, CBD (10 μM) alone or in combination with 3-MA (5 mM). Soft agar colony counts were done by three independent investigators microscopically visualizing individual colonies in 10 random fields. Data shown are the mean ± SD of the percentage of colonies with respect to vehicle obtained in three separate. (*k*) Representative immunoblots of pAKT and AKT in GSCs untreated or treated with CBD (10 μM) for up to 24 hr. GAPDH protein levels were used as loading control. Blots are representative of one of three separate experiments. Numbers represent the densitometric analysis. (*l*) Representative analysis of TRPV2 protein expression in GSCs treated with vehicle, CBD (10 μM) and Ly294002 (1 μM), alone or in combination for 24 hr. Proteins from plasma membrane (M) and cytosolic (C) fractions were immunoblotted with anti-TRPV2 Ab. GAPDH protein levels were used as loading control. Blots are representative of one of three separate experiments. Numbers represent the densitometric analysis. Data shown are relative to GSC #83 line and are representative of the three GSC lines analyzed.

Finally, we also evaluated the effect of CBD-induced autophagy in GSC self-renewal. So, by soft agar assay we confirmed that CBD-induced autophagy affects GSCs proliferation, because a significant reduction of neurosphere formation was observed in CBD- compared with vehicle-treated GSCs, and this effect was reverted by 3-MA (Fig. 2*j*). In addition, since pAKT downregulation is a key signal for activation of autophagic process we evaluated the CBD effects on pAKT. By western blot analysis we evidenced that AKT was phosphorilated in GSC lines and CBD reduced pAKT levels at 6 hr post-treatment, than at later times pAKT returned to basal levels (Fig. 2*k*). Moreover, since the PI3K/AKT pathways have been found to modulate the trafficking of TRPV2 to the cellular membrane, the role of PI3K signaling was further evaluated. GSC lines were treated with LY294002 (PI3K inhibitor, 1μM) and 24 hr post-treatments TRPV2 protein expression was determined by western blot analysis in plasma membrane and cytoplasm fractions. As shown, LY294002 inhibits CBD-induced increase of TRPV2 expression both in the cytosol and plasma membrane (Fig. 2*l*).

CBD promotes the differentiation and sensitizes GSCs to BCNU cytotoxic effects

The effect of CBD in inducing a differentiative phenotype was evaluated by incubating GSC lines in proliferation medium containing EGF and bFGF. CBD effect on modulation of stem cell markers (CD133, Oct-4, SSEA-1, Nestin, Sox2, CXCR4), differentiation markers (GFAP, β_{III}-tubulin) and TRPV2 was evaluated by FACS analysis. As shown, we found that CD133, Oct-4, SSEA-1, Nestin, Sox2 and CXCR4 were expressed although at different levels in GSC lines (Fig. 3*a*). In addition, a significant decrease of CD133, Oct-4, SSEA-1 and Nestin stem cell markers was detected in CDB-treated compared with untreated GSC lines. As shown, CBD reduces the expression of stem cell markers at levels comparable to that found in D-GSC lines (Fig. 3*a*). Moreover, increasing levels of GFAP, β_{III}-tubulin and TRPV2 were evidenced in CDB-treated compared with untreated GSCs, with levels comparable to that found in D-GSC lines (Fig. 3*a*). Next we evaluated if the CBD effect on TRPV2, GFAP and β_{III}-tubulin differentiation markers, was reverted by the autophagic inhibitor 3-MA. As shown, the CBD-induced expression of GFAP, β_{III}-tubulin and TRPV2, was reverted by 3-MA (Fig. 3*b*), suggesting that the CBD-induced autophagy is necessary to induce GSCs differentiation. Stimulation of GSCs differentiation resulted in a reduced resistance of GSCs to BCNU-induced cytotoxic effects.[7] Thus we treated GSCs with BCNU for 48 hr under proliferative condition (medium containing EGF and bFGF) or under differentiative condition (medium containing 5% FBS). We found that GSCs were resistant to BCNU; a slight decrease in cell viability was only observed in BCNU-treated D-GSCs, whereas CBD plus BCNU, in proliferative medium, markedly increases the sensitivity of GSCs to BCNU (Fig. 3*c*). Then, we investigated the mechanisms underlying the increased cytotoxic effect induced by BCNU plus CBD administration. By Annexin-V staining and FACS analysis, a strong increase of the Annexin-V^+ apoptotic cells in BCNU plus CBD-treated GSCs, compared to BCNU- or CBD-treated GSCs was evidenced (Fig. 3*d*). Overall, our results indicate that CBD-induced autophagy represents a prerequisite for BCNU-induced apoptotic cell death.[25] Furthermore, no significative dissipation in mitochondrial transmembrane potential was found in BCNU- or CBD-treated GSCs, whereas a three-fold increase was observed in BCNU plus CBD-treated GSCs (Fig. 3*e*). Since TMZ is frequently used in GBM therapies, we evaluated the TMZ effect in GSC lines. As showed, we found that TMZ has no effects alone or in combination with CBD, in GSC and D-GSC lines (Supporting Information Fig. S5*a* and S5*b*). Moreover, we evidenced that the resistance to TMZ is not correlate with MGMT promoter methylation state, since MGMT promoter in GCS #83 was unmethylated, while in GSC #1 and GSC #30 was hypermethilated (Supporting Information Fig. S5*c*). Overall, CBD inducing GSCs differentiation increases the sensitivity to BCNU cytotoxicity by inducing mitochondrial-dependent apoptosis.

Expression of the Aml-1 spliced variants in GSC and D-GSC lines

The expression of Aml-1a, Aml-1b and Aml-1c was investigated by qualitative PCR in the GSC lines. Results showed three different transcripts of 205, 232 and 168 bp, respectively, corresponding to Aml-1a, Aml-1b and Aml-1c spliced variants in all the GSC lines analyzed (Fig. 4*a*). By qRT-PCR Aml-1a, Aml-1b and Aml-1c relative expression was determined in all the GSC and in D-GSC lines (Figs. 4*b* and 4*c*). As shown, we determined the Aml-1 spliced variant levels and we found that Aml-1a mRNA is overexpressed (at 7 and 14 days of differentiation) in all the D-GSC lines, compared with the respective GSC lines, whereas Aml-1b and Aml-1c display a cell line-specific expression profile (Fig. 4*c*). Since our data demonstrated that CBD induces GSC differentiation, we evaluated the effect of CBD, in regulating Aml-1a expression. By qRT-PCR and western blot analysis we found that CBD increases the Aml-1a mRNA and protein expression compared with vehicle-treated GSCs (Figs. 4*d* and 4*e*). Then, we evaluated the role of CBD-induced TRPV2 activation in regulating Aml-1a expression. GSC lines were treated with RR, tranilast, LY294002 alone and in combination with CBD, and Aml-1a nuclear levels were determined by western blot analysis. As shown, the CBD-induced Aml-1a expression was reduced both by RR, tranilast and LY294002, suggesting the involvement of TRPV2 and PI3K pathways in CBD-induced Aml-1a expression (Fig. 4*e*).

Then, we evaluated if the increase of TRPV2 observed in D-GSCs was under the transcriptional control of Aml-1a. ChIP analysis were performed in GSCs, D-GSCs and in siAml-1 (knock-down of all siAml-1 spliced variants), and siAml-1a silenced D-GSCs. Before ChIP assays, to assess if gene silencing was effective in reducing the three isoforms in

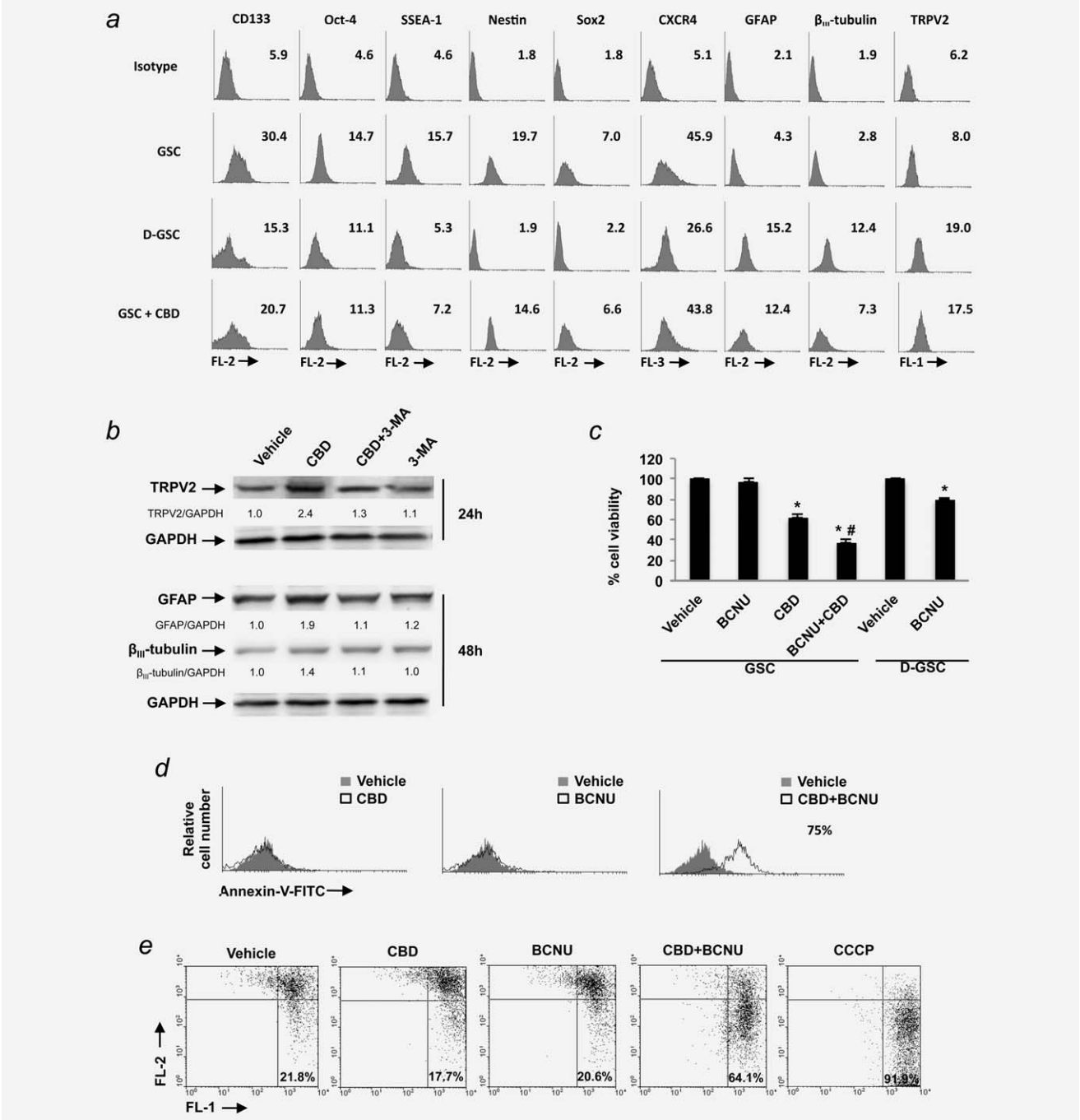

Figure 3. CBD promotes differentiation through the autophagic pathway and increases chemosensitivity of GSCs. (*a*) Untreated or CBD-treated GSCs were cultured in proliferative medium containing EGF and bFGF for 48 hr. D-GSCs were cultured in differentiative medium containing 5% FBS for 72 hr. CD133, Oct-4, SSEA-1, Nestin, Sox2, CXCR4, GFAP, β_{III}- tubulin and TRPV2 expression levels were detected by FACS analysis. Data shown are expressed as mean fluorescence intensity (MFI) and are representative of one of three separate experiments. (*b*) Lysates from GSCs, untreated or treated with 10 μM of CBD pretreated or not with 3-MA (5 mM) for 1 hr, were separated on 7% SDS-PAGE and probed with anti-TRPV2, anti-GFAP and anti-β_{III}-tubulin Abs. Blots are representative of one of three separate experiments. Protein levels were expressed as relative fold respect to GAPDH protein level used as loading control. The values indicate the density proportion of each protein compared with vehicle. (*c*) GSCs were cultured for 24 hr with CBD (10 μM) and BCNU (200 μM) alone or in combination in a proliferative medium. Moreover GSC cells were treated with BCNU (200 μM) or vehicle in a differentiative medium. Cell viability was determined by MTT assay. Data are expressed as mean ± SD. *$p < 0.01$ *vs*. vehicle; #$p < 0.01$ *vs*. CBD-treated cells. (*d*) Percentage of Annexin-V+ cells in GSCs treated with CBD (10 μM), BCNU (200 μM), alone or in combination was determined by FACS analysis. Histograms are representative of one of three separate experiments. Data are expressed as percentage of positive cells. (*e*) Changes of $\Delta\psi$m were evaluated in GSCs treated as above described, by JC-1 staining and biparametrice FL1 (green)/FL2 (red) flow cytometric analysis. Numbers indicate the percentage of cells showing a drop in $\Delta\psi$m-related red fluorescence intensity. CCCP was used as positive control.

siAml-1 D-GSCs and Aml-1a in siAml-1a D-GSCs we evaluated the protein expression of Aml-1 splice variants, in nuclear extracts by western blot. As shown the Aml-1 isoform levels were higher in D-GSCs compared with both GSCs and siAml-1 D-GSCs; moreover only Aml-1a isoform levels were reduced in siAml-1a D-GSCs compared with both D-GSCs and siAml-1 D-GSCs (Fig. 4*f*). siFluo cotransfection was performed to confirm siRNA intake in GSC lines (Supporting Information Fig. S6). So gene silencing results demonstrated the specificity of both siAml-1 and siAml-1a. By ChIP analysis we assessed whether and which Aml-1 isoform direcly contributes to TRPV2 transcription. We found an increase of TRPV2 sites IP fold enrichment in D-GSCs (3.5 (+)01Kb, 5.0 (+)08Kb) compared with GSCs and a decrease

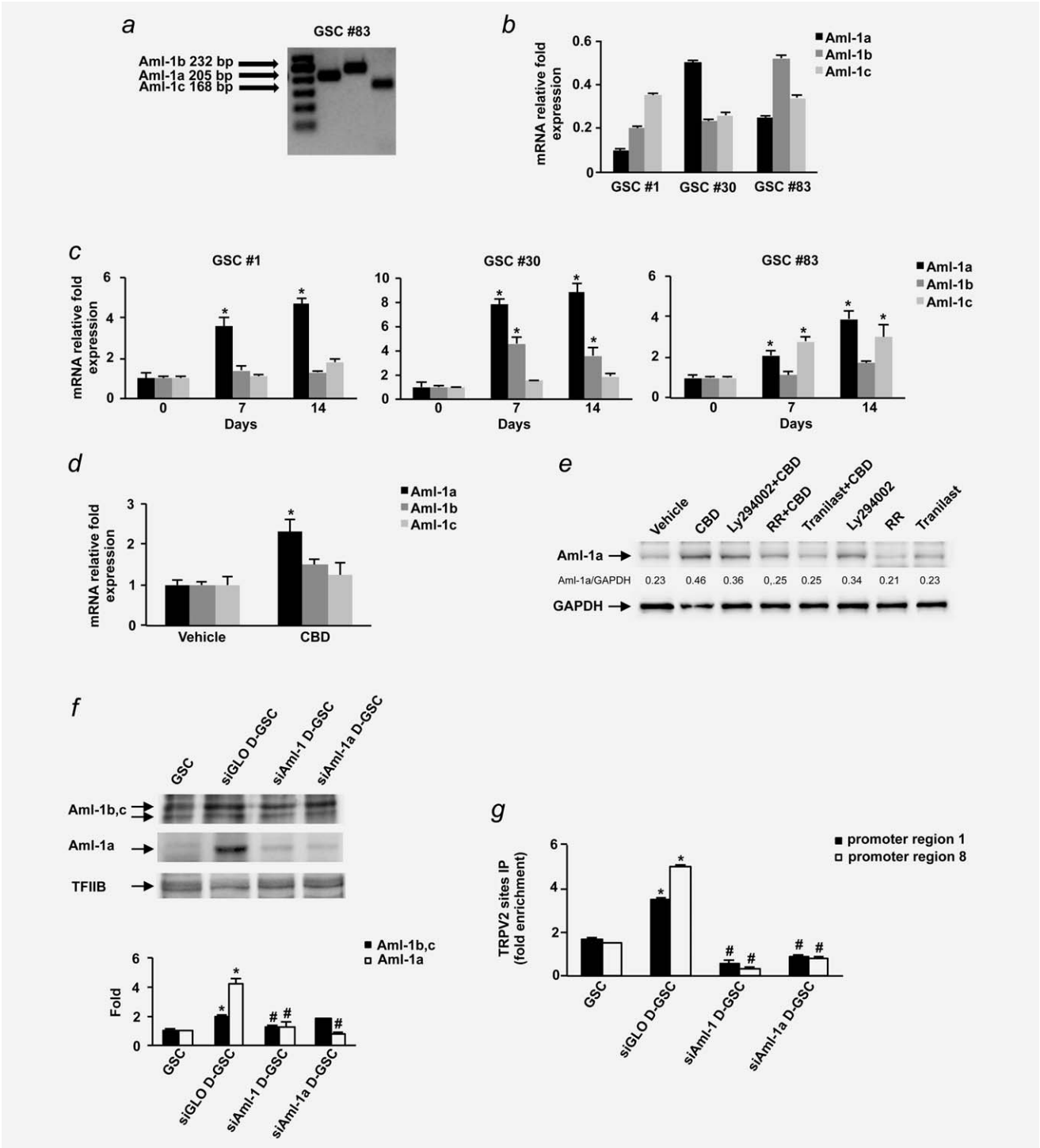

Figure 4:

of these sites in both siAml-1 D-GSCs (0.3 (+)01Kb, 0.8 (+)08Kb) and siAm-1a D-GSCs (0.6 (+)01Kb, 0.9 (+)08Kb; Fig. 4*g*). These results indicated that Aml-1a binds to TRPV2 gene promoters, and this interaction enhances TRPV2 transcription. In fact, TRPV2 site IP fold lower levels were detected during siAml-1 and siAml-1a gene silencing in D-GSCs compared with siGLO D-GSCs, indicating that Aml-1a is the main isoform bound to the TRPV2 promoter region during GSCs differentiation.

Silencing of Aml-1a spliced variant promotes self renewal and proliferation and inhibits the differentiation of GSCs

To demonstrate the involvement of Aml-1a in the modulation of GSCs proliferation and self renewal capability and differentiation, we knock-down the Aml-1a gene during the GSCs differentiation. Transfection with siAml-1a markedly reduced the Aml-1a expression, both at mRNA (about 70%) and protein level (about 60%), evaluated at day 7 of differentiation (Supporting Information Fig. 6). Moreover, by MTT assay, BrdU incorporation and clonogenic assays, we found that silencing of Aml-1a in D-GSCs increases the GSCs viability (Fig. 5*a*), the percentage of $BrdU^+$ cells from 49% to 67% (Fig. 5*b*) and the number of total colonies growth in soft agar compared with siGLO-transfected D-GSCs, respectively (Fig. 5*c*). Moreover, a reduced expression of TRPV2, GFAP and β_{III}-tubulin was found in siAml-1a D-GSC compared with siGLO D-GSC lines (Fig. 5*d*). No changes in Nestin and Sox2 expression were found in siAml-1a- *vs.* siGLO D-GSCs (Fig. 5*d*). In addition, we analyzed the expression of 84 genes involved in signal transduction pathways important for stem cell maintenance, proliferation and/or differentiation, in siAml-1a- and siGLO-transfected D-GSC lines, by a Stem Cell Signaling Pathway Finder PCR array. The results showed that Aml-1a gene silencing in GSCs significantly induces the expression of 5 genes as well as 20 other genes are upregulates (Table 1), suggesting that lost of Aml-1a expression promotes a genetic transcriptional program confering to the D-GSCs a less differentiated stem cell and more proliferative phenotype, indicating that Aml-1a splice variant impairs the proliferation and promotes the differentiation in GSCs.

Discussion

The malignant phenotype of GBM is believed to be largely driven by GSCs, and targeting GSCs is now considered a promising new approach for GBM treatment.[26,27] Cannabinoids have been demonstrated to act as antitumour agents in human GBM cell lines, both *in vitro* and *in vivo*,[11,28] and to decrease the efficiency of GSCs to initiate glioma formation.[14] In particular, CBD has been shown to inhibit survival and proliferation,[24] to induce cell death and chemosensitizing effects in human GBM and other cancer cell lines in a CB receptor-independent and TRPV2-dependent manner.[11,29,30]

Herein, we demonstrated that CBD through TRPV2 activation induces autophagy in GSCs. The autophagy genes activated by CBD include ULK2, Atg9B, ATG10, Beclin-1, GARABAP, ATG16 L2, PI3CG and RAB24 genes. In addition, we found that CBD-induced autophagy in GSCs may be the result of changes in the expression of eukaryotic initiator factors (eIFs) of unfolded protein response. Translation of mRNAs that affect stress-mediated differentiation, cellular growth, apoptosis and autophagy is regulated by the AKT/mTOR protein kinase network and requires the recruitment of the eIF4F complex (the cap-binding protein eIF4E, the scaffolding protein eIF4G and an ATP-dependent RNA helicase eIF4A). Downregulation and upregulation of the eIF4GI and eIF2AK3, respectively were found in CBD-treated GSCs.

Autophagy activation *via* the CBD/TRPV2 pathway inhibited viability and proliferation, arrested the cell cycle at the G0/G1 phase and promoted the activation of a differentiation program as evaluated by the increase of the expression of GFAP and β_{III}-tubulin differentiation markers in GSCs. These effects were inhibited by the cotreatment with autophagic blockers, suggesting that CBD induces differentiation of GSCs throught the autophagic pathway. Similarly, the autophagic activator, rapamycin promotes differentiation of glioma stem/progenitor cells (GSPGs), and 3-MA and BAF1 inhibited the FBS-induced differentiation of GSPGs.[9]

Figure 4. Aml-1a expression increases during GSCs differentiation and binds TRPV2 promoter. (*a*) Representative agarose gel electrophoresis of Aml-1 isoforms mRNA expression evaluated by qualitative PCR in GSC #83 line. (*b*) The relative Aml-1 isoforms mRNA expression in GSCs #1, #30 and #83 was evaluated by qRT-PCR. Aml-1 mRNA levels were normalized for β-actin expression. Data are expressed as mean ± SD. (*c*) Aml-1 isoforms mRNA expression in D-GSC lines (day 7 and 14 of differentiation) was evaluated by qRT-PCR and was expressed as relative fold with respect to the corresponding GSC lines used as calibrator. Data are expressed as mean ± SD; $*p < 0.01$ D-GSCs *vs*. GSCs. (*d*) Aml-1 isoforms mRNA expression in 24 hr vehicle- and CBD-treated GSCs was evaluated by qRT-PCR and was expressed as relative fold with respect to vehicle-treated cells. Data are expressed as mean ± SD; $*p < 0.01$ CBD- *vs*. vehicle-treated. (*e*) Lysates from GSCs treated with vehicle, CBD (10 μM) pretreated or not with RR (10 μM), tranilast (50 μM) or LY294002 (1 μM) for 1 hr, were separated on 10% SDS-PAGE and probed with anti-Aml-1 and anti-GAPDH Abs. Blots are representative of one of three separate experiments. Numbers represent the densitometric analysis. (*f*) Nuclear fractions from GSCs and from siGLO D-GSCs, siAml-1 D-GSCs and siAml-1a D-GSCs at day 7 of differentiation were immunoblotted with Aml-1 Ab and the relative isoforms protein levels were determined using TFIIB protein levels as loading control. To detect Aml-1b,c and Aml-1a variants, 10% and 12% SDSPAGE gels were performed, respectively. Blots shown are representative of one of three separate experiments. Bar graphs represent the mean ± SD of at least three separate experiments, $*p < 0.01$ *vs*. GSCs; $\#p < 0.01$ *vs*. iGLO D-GSCs. (*g*) ChIP analysis of GSCs and of siGLO D-GSCs, siAml-1 D-GSCs and siAml-1a D-GSCs cultured for 7 days in differentiation conditions. DNA immunoprecipitated by using Aml-1 Ab directed against all three isoforms was amplified by qRT-PCR. Data are expressed as mean ± SD of three independent experiments, $*p < 0.01$ *vs*. GSCs, $\#p < 0.01$ *vs*. iGLO D-GSCs. Data shown are relative to GSC #83 line and are representative of the three GSC lines analyzed.

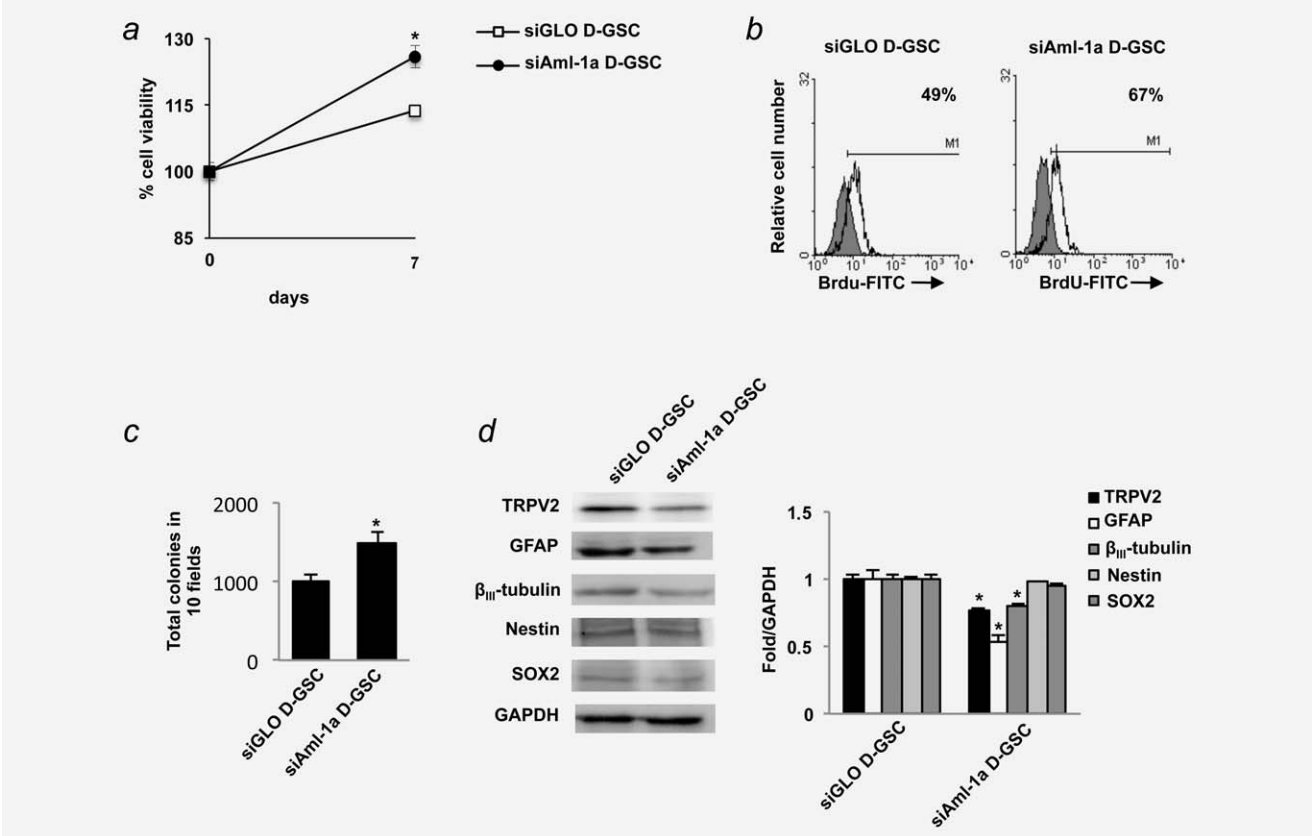

Figure 5. Aml-1a regulates proliferation and differentiation of GSCs. (*a*) siGLO and siAml-1a GSCs were cultured up to 7 days under differentiation conditions (D-GSCs). Cell viability was determined by MTT assay. Data shown are expressed as mean ± SD of three separate experiments; $*p < 0.01$ *vs*. siGLO D-GSCs. (*b*) siGLO and siAml-1a D-GSCs were cultured as above described and proliferation was assessed by the BrdU incorporation assay. BrdU was added 24 hr before the harvesting of cells. Cells were stained for BrdU incorporation and analyzed by FACS. The position of M1 (BrdU+ marker) was determined by a BrdU(-) control, dark curve. Percentages indicate the number of cells that are positive for BrdU in the total sample size. (*c*) siGLO and siAml-1a D-GSCs were grown in soft agar for 14 days. Soft agar colony counts were done by three independent investigators microscopically visualizing individual colonies in 10 random fields. Data shown are the mean ± SD of colony counts obtained in three separate experiments. $*p < 0.01$ *vs*. siGLO DGSCs. (*d*) Immunoblots of TRPV2, GFAP, β_{III}-tubulin, Nestin and SOX2 protein expression in siGLO D-GSCs and siAml-1a D-GSCs. GAPDH protein levels were used as loading control. Bar graphs represent the mean ± SD of at least three separate experiments, $*p < 0.01$ *vs*. siGLO D-GSCs. Data shown are relative to GSC #83 line and are representative of the three GSC lines analyzed.

The autophagy promoting activity of CBD in GSCs seems to be regulated by the AKT-PI3k/RPS6KBI/PTEN pathway. In fact, downregulation of the prosurvival kinase AKT, and upregulation of PTEN, the negative controller of AKT activity and of PIK3CG kinase were found in CBD-treated GSCs. Moreover, the AKT/mTOR network positively regulates the activity of the mTORC1 complex and AKT inhibition decreases mTORC1 activity and promotes autophagy.[31] Herein, we found that CBD reduces AKT activity in GSC lines, by decreasing pAKT levels, further supporting the role of CBD in regulating autophagy in GSC lines.

Specific markers of autophagic process were LC3 conversion to LC3-II that correlate with the number of autophagosomes and Beclin-1/PI3K-III complex that is involved in the formation of autophagosomes.[9] Furthermore, Beclin-1 was found to confer both autophagy and differentiation in cancer cells.[8] The increase of PIK3CG and LC3-II/LC3-I ratio levels in CBD-treated GSCs, strongly supports for the Beclin-1-PIK3C3 complexes formation, required for the recruitment of autophagic effectors.[32] This evidence was supported in siBeclin-1 GSC lines where CBD effect on cell viability was reverted. Moreover, a decrease of pAKT levels evidenced in CBD-treated GSC lines correlates with activation of autophagic process.

Autophagic pathways induces differentiation in GSC lines, and autophagic inhibitors stimulates GSCs differentiation.[9] Herein, we evidenced that CBD *via* activation of autophagy induces expression of differentiation markers as GFAP,[14] β_{III}-tubulin[14] and decreases expression of stem cell markers as CD133,[33] Oct-4,[34], SSEA-1[35] and Nestin.[14]

Several reports have studied the therapeutic effect of the use of pro-differentiating agents on GSCs, because of their capability to elicit chemosensitizing effects and increment the susceptibility of GSCs to drug cytotoxic.[8] Previous studies

Table 1. siAml-1a influences stem cell signaling pathway

Gene symbol	Fold	SD	Gene symbol	Fold	SD
ACVR1	1.0	0.20	**LTBP4**	**4.8**	**0.12**
ACVR1B	1.0	0.20	NCSTN	1.4	0.11
ACVR1C	1.0	0.30	NFAT5	1.8	0.11
ACVR2A	**16.5**	**0.10**	NFATC1	2.1	0.12
ACVR2B	1.5	0.30	NFATC2	1	0.11
ACVRL1	1.0	0.30	NFATC3	1.2	0.11
AMHR2	1.0	0.20	NFATC4	1.8	0.12
BCL9	1.8	0.30	NOTCH1	1.7	0.10
BCL9L	1.9	0.30	**NOTCH2**	**4.5**	**0.13**
BMPR1A	**5.8**	**0.12**	**NOTCH3**	**11.5**	**0.14**
BMPR1B	1.0	0.20	NOTCH4	2.1	0.10
BMPR2	1.0	0.22	PSEN2	1.7	0.11
CDX2	1.0	0.25	PSENEN	1.2	0.11
CREBBP	2.5	0.13	PTCH1	1.6	0.11
CTNNB1	**2.6**	**0.12**	PTCHD2	1	0.09
E2F5	1.0	0.29	PYGO2	1	0.11
ENG	1.0	0.29	**RBL1**	**3.3**	**0.13**
EP300	2.3	0.40	RBL2	1.8	0.10
FGFR1	**3.4**	**0.18**	RBPJL	1	0.11
FGFR2	induced (1.8)*	0.13	RGMA	1.5	0.08
FGFR3	**induced (3.3)***	**0.10**	SMAD1	1.4	0.10
FGFR4	**induced (3.2)***	**0.11**	SMAD2	1.5	0.12
FZD1	**3.7**	**0.11**	SMAD3	2.1	0.12
FZD2	1	0.11	SMAD4	2.0	0.12
FZD3	**6.2**	**0.11**	SMAD5	2.7	0.15
FZD4	1.5	0.10	**SMAD6**	**5.3**	**0.14**
FZD5	1	0.11	SMAD7	2.0	0.16
FZD6	**5.3**	**0.13**	**SMAD9**	**5.9**	**0.18**
FZD7	2.2	0.14	SMO	1.3	0.09
FZD8	2.5	0.10	SP1	1.3	0.11
FZD9	1	0.20	STAT3	2.0	0.10
GLI1	induced (2.2)*	0.11	SUFU	1.9	0.13
GLI2	**induced (2.8)***	**0.11**	TCF7	2.2	0.16
GLI3	**4.4**	**0.10**	**TCF7L1**	**3.3**	**0.12**
IL6ST	**3.6**	**0.11**	**TCF7L2**	**3.7**	**0.11**
LEF1	2.2	0.12	TGFBR1	1.8	0.10
LIFR	**6.5**	**0.11**	TGFBR2	1	0.10
LRP5	1	0.11	TGFBR3	1.6	0.09
LRP6	1.8	0.11	TGFBRAP1	1.3	0.08
LTBP1	1	0.11	VANGL2	1.9	0.10
LTBP2	2.2	0.12	**ZEB2**	**4.0**	**0.11**
LTBP3	1.5	0.10			

Stem Cell Signaling Pathway Finder PCR array in mRNA samples extracted from siGLO D-GSCs and siAml-1a D-GSCs after 7 days of culture. Values represent fold differences of individual gene expression in siAml-1a D-GSCs compared to siGLO D-GSCs. The expression levels were normalized to the average Ct value of two housekeeping genes (GAPDH and RPLP0) and calculated by the ΔΔCt method. Genes, whose expression is, at least, 2.5-fold upregulated, are in bold.
Data shown are relative to GSC #83 line and are representative of the three GSC lines analyzed.

demonstrated that GSCs are resistant to conventional chemotherapeutic drugs as BCNU.[7] In addition, treatments to increase the differentiation GSCs status result in an higher sensitivity of GSCs to chemotherapeutical drugs.[36] CBD treatments increase BCNU and TMZ chemosensitivity in GBM cell lines and combined administration of THC or THC plus CBD with TMZ synergistically reduces the growth of glioma xenografts.[27] Herein, we found that treatment of GSC with CBD alone doesn't induce apoptosis, but it sensitizes GSCs to BCNU-induced apoptosis. Concordingly downregulation of BCL-XL and CTDS mRNAs involved in drug resistance in GBM, and upregulation of BAD and BAX mRNAs restoring the sensitivity to apoptotic stimuli and increasing the sensitivity to chemotherapy in certain glioma cell types,[37] were found in CBD-treated GSCs. About TMZ, we confirm, as previously reported[7,38] that GSCs are resistant to TMZ chemotherapy.

Aml-1 proteins have been shown as crucial transcription factors influencing a wide range of biological processes, by regulating signaling pathways involved in self renewal, cell proliferation and differentiation.[17]. Herein, we found that all the Aml-1a, Aml-1b and Aml-1c spliced variants analyzed are expressed, although at different level, in the three GSCs lines, but only the Aml-1a variant is upregulated in all the GSC lines analyzed, with a marked accumulation of the Aml-1a protein at nuclear level after GSC differentiation. Treatment of GSCs with CBD, that increases TRPV2 expression, induces Aml-1a mRNA upregulation, suggesting that CBD-induced effects on GSCs differentiation could be partially the result of a CBD-induced Aml-1a transcription. Although Aml-1 has been shown to be critically in maintenance of progenitor cells as well as in their differentiation, the contribute of Aml-1a, as respect to the other spliced variants is not yet fully understood.[17] Aml-1a plays a role in erythroid and megakaryocytic differentiation[39]; in myeloid cells, Aml-1a by repressing the transcription of the macrophage colony-stimulating factor receptor mediated by Aml-1b, blocked the differentiation.[40] We previously demonstrated that TRPV2 over-expression promotes differentiation and inhibits proliferation in GSCs,[11] but the transcriptional regulation of

TRPV2 gene in GSCs was not investigated. Since, Aml-1 (although no information about which spliced variant is involved) has been found to increase expression of several ion channels as TRPV1, TRPA1 and TRPM8,[41] we evaluated if Aml-1a was involved in TRPV2 transcription. So by CHIP analysis in siAml-1 and in siAml-1a transfected D-GSCs we demonstrated that TRPV2 upregulation in D-GSC lines requires Aml-1a, since its abrogation reduces TRPV2 promoters activity resulting in downregulation of TRPV2 expression levels.

Silencing of Aml-1a during GSC differentiation stimulates self renewal capability, with an increased total colony numbers, enhances cell viability and proliferation, and reduces the expression of the GFAP, β_{III}-tubulin and TRPV2 differentiation markers, whereas no changes of Sox2 and Nestin were found. Thus, Aml-1a silencing of at day 7 of differentiation strongly inhibits GSCs astroglial differentiation promoting GSCs proliferation, stemness and pluripotency. These processes are defined by number of key signal transduction pathways that are regulated by a stem cell transcription factors. Here, we found that Aml-1a silencing activates a mitogenic signaling pathways in GSCs. Thus, FGFR2, FGFR3 and FGFR4 and GLI1 and GLI2 glioma-associated transcription genes belonging to FGF and Hedgehog pathways were *ex-novo* induced. FGF and EGF are the main recombinant growth factor in GSC medium.[42] Gli1, Gli2 and Gli3 are executers of Sonic Hedgehog (Shh) signaling and targets the TGFβ signaling axis.[43] They are indispensable for glioma-initiating cells (GICs) proliferation and Shh inhibitors prevented GIC proliferation. Increased NOTCH2/3 mRNA expression was found in siAml-1a GSCs. Activation of NOTCH signaling in GSCs enhanced colony formation capability and increased self-renawal and dedifferentiation; in particular, NOTCH3 stimulates glioma cell proliferation, cell migration, invasion and apoptosis.[44] Increased proliferation observed in siAml-1a GSCs is also the result of upregulation of ACVR2A, BMPR1A, LTBP4 and SMAD6,9 belonging to BMP and TGFβ superfamily. ACVR2A regulates proliferation in neurosensory tissues.[45] BMP/BMPR1A/B pathway inhibits the differentiation of glioblastoma tumor initiating cells.[46] Latent transforming growth factor binding proteins (LTBPs) are involved in the regulation of mesenchymal cell functions[47] and TGFβ biodisponibility.[48] Wnt/frizzled (FZD) cascades control cell fate, proliferation and migration. A high level of CTNNB1 (Wnt/β-catenin), its frizzled receptors FZD1, FZD3 and FZD6[49] and the β-catenin coactivators TCFL1 and TCFL2 which increase GBM proliferation,[50] were found in siAml1-a GSCs. We also found that both IL-6ST/gp130 and LIFR implicated in GSC pluripotency mainteinance and self-renewal[51] and the vertebrate zinc finger E-box binding homeobox-2 (ZEB2), that suppresses the E-cadherin expression and differentiation as well as stimulates proliferation, migration and invasion,[52] were upregulated in siAml-1a GSCs.

In summary, in this study we identify a potential new pathway that links the activation of autophagy to differentiation, which promotes molecular events that sensitize GSCs to the apoptotic death. Moreover, a relevant role was ascribed to Aml-1a variant in the induction of GSC differentiation. Therefore, understanding of the exact mechanism of Aml-1 variants implicated in the regulation GSC self-renewal, proliferation and differentiation will provide tools for the development of more successful therapeutic strategies.

References

1. Wilson TA, Karajannis MA, Harter DH. Glioblastoma multiforme: state of the art and future therapeutics. *Surg Neurol Int* 2014;5:64
2. Alderton GK. Tumorigenesis: the origins of glioma. *Nat Rev Cancer* 2011;11:627
3. Kesari S. Understanding glioblastoma tumor biology: the potential to improve current diagnosis and treatments. *Semin Oncol* 2011;38:S2–10.
4. Nduom EK, Hadjipanayis CG, Van Meir EG. Glioblastoma cancer stem-like cells: implications for pathogenesis and treatment. *Cancer J* 2012;18:100–106.
5. Ahmed A, Auffinger B, Lesniak MS. Understanding glioma stem cells: rationale, clinical relevance and therapeutic strategies. *Expert Rev Neurother* 2013;13:545–555.
6. Bayin NS, Modrek AS, Placantonakis DG. Glioblastoma stem cells: molecular characteristics and therapeutic implications. *World J Stem Cells* 2014;6:230–238.
7. Gong X, Schwartz PH, Linskey ME, et al. Neural stem/progenitors and glioma stem-like cells have differential sensitivity to chemotherapy. *Neurology* 2011;76:1126–1134.
8. Zhuang W, Li B, Long L, et al. Induction of autophagy promotes differentiation of glioma-initiating cells and their radiosensitivity. *Int J Cancer* 2011;129:2720–2731.
9. Zhao Y, Huang Q, Yang J, et al. Autophagy impairment inhibits differentiation of glioma stem/progenitor cells. *Brain Res.* 2010;1313:250–258.
10. Salazar M, Carracedo A, Salanueva IJ, et al. Cannabinoid action induces autophagy-mediated cell death through stimulation of ER stress in human glioma cells. *J Clin Invest* 2009;119:1359–1372.
11. Nabissi M, Morelli MB, Santoni M, et al. Triggering of the trpv2 channel by cannabidiol sensitizes glioblastoma cells to cytotoxic chemotherapeutic agents. *Carcinogenesis* 2013;34:48–57.
12. Galve-Roperh I, Chiurchiù V, Díaz-Alonso J, et al. Cannabinoid receptor signaling in progenitor/stem cell proliferation and differentiation. *Prog Lipid Res* 2013;52:633–650.
13. Aguado T, Carracedo A, Julien B, et al. Cannabinoids induce glioma stem-like cell differentiation and inhibit gliomagenesis. *J Biol Chem* 2007;282:6854–6862.
14. Morelli MB, Nabissi M, Amantini C, et al. The transient receptor potential vanilloid-2 cation channel impairs glioblastoma stem-like cell proliferation and promotes differentiation. *Int J Cancer* 2012;131:E1067–77. 10.
15. Cooper LA, Gutman DA, Chisolm C, et al. The tumor microenvironment strongly impacts master transcriptional regulators and gene expression class of glioblastoma. *Am J Pathol* 2012;180:2108–2119.
16. Sumazin P, Yang X, Chiu HS, et al. An extensive microRNA-mediated network of RNA-RNA interactions regulates established oncogenic pathways in glioblastoma. *Cell* 2011;147:370–381.
17. Chuang LS, Ito K, Ito Y. RUNX family: regulation and diversification of roles through interacting proteins. *Int J Cancer* 2013;132:1260–1271.
18. Harada H, Harada Y, Niimi H, et al. High incidence of somatic mutations in the aml1/runx1 gene in myelodysplastic syndrome and low blast percentage myeloid leukemia with myelodysplasia. *Blood* 2004;103:2316–2324.
19. Hatlen MA, Wang L, Nimer SD. AML1-ETO driven acute leukemia: insights into pathogenesis and potential therapeutic approaches. *Front Med* 2012;6:248–262.
20. Ferrari N, Mohammed ZM, Nixon C, et al. Expression of runx1 correlates with poor patient prognosis in triple negative breast cancer. *PLoS One* 2014;9:e100759.

21. Sakakura C, Hagiwara A, Miyagawa K, et al. Frequent downregulation of the runt domain transcription factors runx1, runx3 and their cofactor CBFB in gastric cancer. *Int J Cancer* 2005;113: 221–228.
22. Chen CL, Broom DC, Liu Y, et al. Runx1 determines nociceptive sensory neuron phenotype and is required for thermal and neuropathic pain. *Neuron* 2006;49:365–377.
23. Ugarte GD, Diaz E, Biscaia M, et al. Transcription of the pain-related trpv1 gene requires runx1 and C/EBPβ factors. *J Cell Physiol* 2013;228:860–870.
24. Klionsky DJ, Abdalla FC, Abeliovich H, et al. Guidelines for the use and interpretation of assays for monitoring autophagy. *Autophagy* 2012;8:445–544.
25. Huang Z, Cheng L, Guryanova OA, et al. Cancer stem cells in glioblastoma–molecular signaling and therapeutic targeting. *Protein Cell* 2010;1:638–655.
26. Kang MK, Kang SK. Tumorigenesis of chemotherapeutic drug-resistant cancer stem-like cells in brain glioma. *Stem Cells Dev* 2007;16:837–847.
27. Torres S, Lorente M, Rodríguez-Fornés F, et al. A combined preclinical therapy of cannabinoids and temozolomide against glioma. *Mol Cancer Ther* 2011;10:90–103.
28. Shrivastava A, Kuzontkoski PM, Groopman JE, et al. Cannabidiol induces programmed cell death in breast cancer cells by coordinating the cross-talk between apoptosis and autophagy. *Mol Cancer Ther* 2011;10:1161–1172.
29. Morelli MB, Offidani M, Alesiani F, et al. The effects of cannabidiol and its synergism with bortezomib in multiple myeloma cell lines. A role for transient receptor potential vanilloid type-2. *Int J Cancer* 2014;134:2534–2546.
30. Ramirez-valle F, Braunstein S, Zavadil J, et al. eIF4GI links nutrient sensing by mTOR to cell proliferation and inhibition of autophagy. *J Cell Biol* 2008;181:293–307.
31. Guertin DA, Sabatini DM. Defining the role of mTOR in cancer. *Cancer Cell* 2007;12:9–22.
32. Wirth M, Joachim J, Tooze SA. Autophagosome formation-the role of ulk1 and Beclin1-pi3kc3 complexes in setting the stage. *Semin Cancer Biol* 2013;23:301–309.
33. Brescia P, Ortensi B, Fornasari L, et al. Cd133 is essential for glioblastoma stem cell maintenance. *Stem Cells* 2013;31:857–869.
34. Kobayashi K, Takahashi H, Inoue A, et al. Oct-3/4 promotes migration and invasion of glioblastoma cells. *J Cell Biochem* 2012;113:508–517.
35. Son MJ, Woolard K, Nam DH, et al. SSEA-1 is an enrichment marker for tumor-initiating cells in human glioblastoma. *Cell Stem Cell* 2009;4: 440–452.
36. Binello E, Germano IM. Targeting glioma stem cells: a novel framework for brain tumors. *Cancer Sci* 2011;102:1958–1966.
37. Lytle RA, Jiang Z, Zheng X, et al. BCNU downregulates anti-apoptotic proteins bcl-xL and Bcl-2 in association with cell death in oligodendroglioma-derived cells. *J Neurooncol.* 2004;68:233–241.
38. Auffinger B, Tobias AL, Han Y, et al. Conversion of differentiated cancer cells into cancer stem-like cells in a glioblastoma model after primary chemotherapy. *Cell Death Differ* 2014;21:1119–1131.
39. Niitsu N, Yamamoto-Yamaguchi Y, Miyoshi H, et al. AML1a but not AML1b inhibits erythroid differentiation induced by sodium butyrate and enhances the megakaryocytic differentiation of k562 leukemia cells. *Cell Growth Differ* 1997;8: 319–326.
40. Liu X, Zhang Q, Zhang DE, et al. Overexpression of an isoform of aml1 in acute leukemia and its potential role in leukemogenesis. *Leukemia* 2009; 23:739–745.
41. Liu Y, Ma Q. Generation of somatic sensory neuron diversity and implications on sensory coding. *Curr Opin Neurobiol* 2011;21:52–60.
42. Loilome W, Joshi AD, ap Rhys CM, et al. Glioblastoma cell growth is suppressed by disruption of fibroblast growth factor pathway signaling. *J Neurooncol* 2009;94:359–366.
43. Piirsoo A, Kasak L, Kauts ML, et al. Protein kinase inhibitor su6668 attenuates positive regulation of gli proteins in cancer and multipotent progenitor cells. *Biochim Biophys Acta* 2014;1843: 703–714.
44. Kristoffersen K, Villingshøj M, Poulsen HS, et al. Level of notch activation determines the effect on growth and stem cell-like features in glioblastoma multiforme neurosphere cultures. *Cancer Biol Ther* 2013;14:625–637.
45. Chen YG, Wang Q, Lin SL, et al. Activin signaling and its role in regulation of cell proliferation, apoptosis, and carcinogenesis. *Exp Biol Med* 2006; 231:534–544.
46. Lee J, Son MJ, Woolard K, et al. Epigenetic-mediated dysfunction of the bone morphogenetic protein pathway inhibits differentiation of glioblastoma-initiating cells. *Cancer Cell* 2008;13: 69–80.
47. Davis MR, Andersson R, Severin J, et al. Transcriptional profiling of the human fibrillin/LTBP gene family, key regulators of mesenchymal cell functions. *Mol Genet Metab* 2014;112:73–83.
48. Kretschmer C, Conradi A, Kemmner W, et al. Latent transforming growth factor binding protein 4 (LTBP4) is downregulated in mouse and human DCIS and mammary carcinomas. Cell Oncol 2011;34:419–434.
49. Huang HC, Klein PS. The frizzled family: receptors for multiple signal transduction pathways. *Genome Biol* 2004;5:234
50. Halatsch ME, Löw S, Mursch K, et al. Candidate genes for sensitivity and resistance of human glioblastoma multiforme cell lines to erlotinib. Laboratory investigation. *J Neurosurg* 2009;111:211–218.
51. Peñuelas S, Anido J, Prieto-Sánchez RM, et al. TGF-beta increases glioma-initiating cell self-renewal through the induction of LIF in human glioblastoma. *Cancer Cell* 2009;15:315–327.
52. Qi S, Song Y, Peng Y, et al. Zeb2 mediates multiple pathways regulating cell proliferation, migration, invasion, and apoptosis in glioma. *PLoS One* 2012;7:e38842.